JOURNAL OF APPLIED ELECTROCHEMISTRY 19 (1989) 255–262

# Hydrogen evolution on iridium oxide cathodes

J. C. F. BOODTS*, S. TRASATTI†

*Department of Physical Chemistry and Electrochemistry, University of Milan, Via Venezian 21, 20133 Milan, Italy*

Received 21 June 1988; revised 15 August 1988

$IrO_x$ electrodes prepared by thermal decomposition of $IrCl_3$ dissolved in water have been prepared at temperatures betweeen 300 and 500° C. They have been characterized by voltammetric curves before and after each experiment to monitor changes in surface conditions. Hydrogen evolution from 1 mol $dm^{-3}$ constant ionic strength perchlorate solutions at pH between 0 and 1 has been studied by quasi-stationary potentiostatic curves and reaction order determination. A Tafel slope close to 40 mV and a reaction order of 1.5 with respect to $H^+$ are explained with a mechanism involving a step of reduction of the active sites and a pH dependence of the potential at the reaction plane which is typical of the acid–base properties of oxide surfaces. The results indicate that wetting–dewetting phenomena of the electrode surface, depending on the magnitude of the current, are operative during hydrogen evolution, and that the oxide surface is never reduced down to the metal, while no bulk reduction whatsoever takes place.

## 1. Introduction

Apart from the direct electrolytic production, hydrogen evolution is the cathode reaction accompanying, in particular, chlorine formation, and in general most of the anodic processes occurring in aqueous media. Therefore its energetics influence the electrolysis parameters of the whole cell.

In the search for new materials and for new applications of technologically established materials, recent patents have claimed good performances for oxide electrodes for the cathodic evolution of hydrogen [1–3]. It appears that the most interesting feature is not the electrocatalytic activity itself but rather the resistance to deactivation due to the deposition of metallic impurities polluting technical solutions.

As often happens, applications have anticipated fundamental understanding. There are, in fact, only two papers in the open literature [4, 5] dealing with kinetic aspects of hydrogen evolution at oxides. Actually, the first work due to one of us [4] was carried out long before any practical application was envisaged. In that study, some Tafel lines for $H_2$ liberation at $RuO_x$ electrodes were reported but no complete mechanistic and stability investigation was performed. Recently, $RuO_x$ has been compared to Pt and Ru for its ability to remain active for $H_2$ evolution even in the presence of metallic impurities [5]. The observed weak adsorption of metals (no underpotential deposition) has been attributed to a different surface chemistry which, however, has not been specified.

Two more publications are to be mentioned dealing with the cathodic behaviour of $RuO_2$ [6] and $IrO_2$ [7] single crystals in the region of hydrogen adsorption. However they do not report any kinetic data for the evolution reaction.

The most intriguing aspect of oxide cathodes is that they are, in principle, thermodynamically unstable in the hydrogen adsorption region [8] and are thus not expected to be good cathodes. Fundamental research should find an answer to such a crucial question. A prerequisite is that the details of the kinetic mechanism and of the surface response should be known.

While the very few available kinetic data refer to the behaviour of $RuO_x$, no information whatsoever is available on the performance of $IrO_x$ as a cathode, despite its widespread use as a component of oxide electrodes in technological applications. Since this oxide is particularly stable in acid solution [9], this work starts a series of systematic investigations on the cathodic behaviour of oxides by studying the kinetic mechanism of hydrogen evolution from acid solutions using thermally prepared $IrO_x$.

## 2. Experimental details

The following experimental studies were performed: voltammetric curves, quasi-stationary potentiostatic curves and reaction order determination. AMEL instrumentation was used throughout the work.

### 2.1. *Electrodes*

These were prepared by depositing a layer of $IrO_x$ on both sides of 10 × 10 × 0.2 mm Ti plates. The precursor was $IrCl_3 \cdot nH_2O$ (Ventron) dissolved in water and spread onto the support by brush. The plates were then fired for 10 min at the selected temperature

* Visiting scientist from the University of São Paulo at Ribeirão Preto, Brazil.
† To whom correspondence should be addressed.

0021-891X/89 $03.00 + .12 

in an oxygen stream. The operation was repeated until the desired amount of catalyst was achieved (*ca* 2.4 mg cm$^{-2}$, for a nominal thickness of 2 $\mu$m). The samples were finally annealed for 1 h at the same temperature. Calcination was carried out at the following temperatures: 300, 330, 360, 400, 450 and 500° C. Two samples were prepared at each temperature.

The special Teflon holder for the electrodes and the electrolysis cell have been described previously [10, 11].

### 2.2. *Solutions*

1 mol dm$^{-3}$ $HClO_4$ (Fluka, purum p.a.) solutions were used for most of the experiments. These were prepared volumetrically with doubly distilled water. In the experiments for the determination of the reaction order, solutions at 1 mol dm$^{-3}$ constant ionic strength were used by adding the necessary amount of $NaClO_4$ (Fluka, purum p.a.), used without further purification, to $HClO_4$ solutions in the range 0.1–1 mol dm$^{-3}$.

### 2.3. *Potentials*

All potentials were measured and are reported against a hydrogen electrode in the same solution (RHE) obtained by bubbling hydrogen at atmospheric pressure around a platinized Pt wire suitably activated before use.

### 2.4. *Experimental procedures*

Voltammetric curves were recorded at 20 mV s$^{-1}$ in the potential range 0.4–1.4 V vs RHE, as a rule after a few cycles to obtain stable profiles. No detectable drift was observed with time for suitably conditioned electrodes. Voltammetric charges ($q^*$) were determined by means of a graphical integrator directly on the recorded curves [12]. $q^*$ was used as a sensitive parameter to monitor variations in the surface state of electrodes [13]. Charges were recorded for the fresh electrodes, and again after each set of experiments. At a certain time the electrodes were separated into two groups: one set was stored in air, another in water. This was in order to investigate the effect of the ambient conditions on the value of $q^*$.

Potentiostatic experiments were performed by first conditioning the electrode at 0.2 V for 15 min, then moving the potential down to 0 V by 50-mV steps, and further to more negative values by 10-mV steps. The current was read after 3 min at each potential. Before taking the electrodes out of the solution they were reconditioned for 10 min at 0.4 V.

The reaction order was determined by measuring the current at a single constant potential for several pHs. All electrodes were used in the same solution at a given pH before changing the composition. In this way the effect of the previous history of the surface was minimized. Potential–time sequences were as follows: 0.4 V (5 min) → 0.2 V (5 min) → selected $E$. The current was read after 7 min.

In order to check whether hydrogen predischarge may influence the mechanism, the order of reaction was also determined using the following potential sequence: 0.4 V (5 min) → −0.2 V (5 min) → selected $E$. The selected $E$ was −0.01 V for the forward sequence and 0 V for the backward.

Ohmic drops were estimated indirectly by first drawing the low-overpotential Tafel line up to the highest current density and then measuring the $\Delta E$ at constant current between the experimental points and the extended straight line. In the case of deviations purely due to ohmic drops, the plot of $\Delta E$ vs $j$ must result in a strictly linear dependence going through the origin of the axes. Should the deviations also involve a transition to a higher Tafel slope, no linearity can be observed in $\Delta E$ vs $j$ plots.

## 3. Results and discussion

Hydrogen evolution from $HClO_4$ solutions may be accompanied by some perchlorate reduction. This

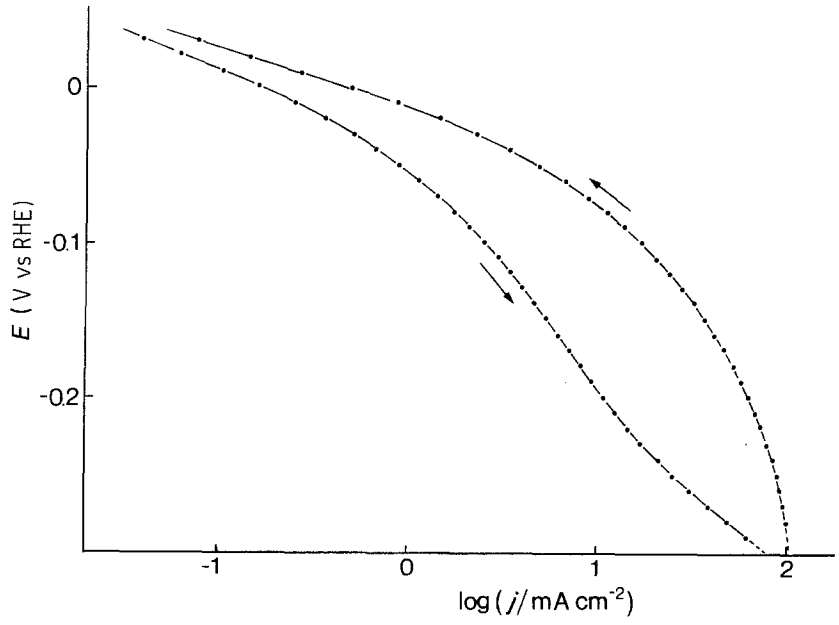


Fig. 1. Typical $E$–log $j$ curve for hydrogen evolution on $IrO_x$ from $HClO_4$ solution showing a remarkable hysteresis between forward and backward direction of potential scanning.

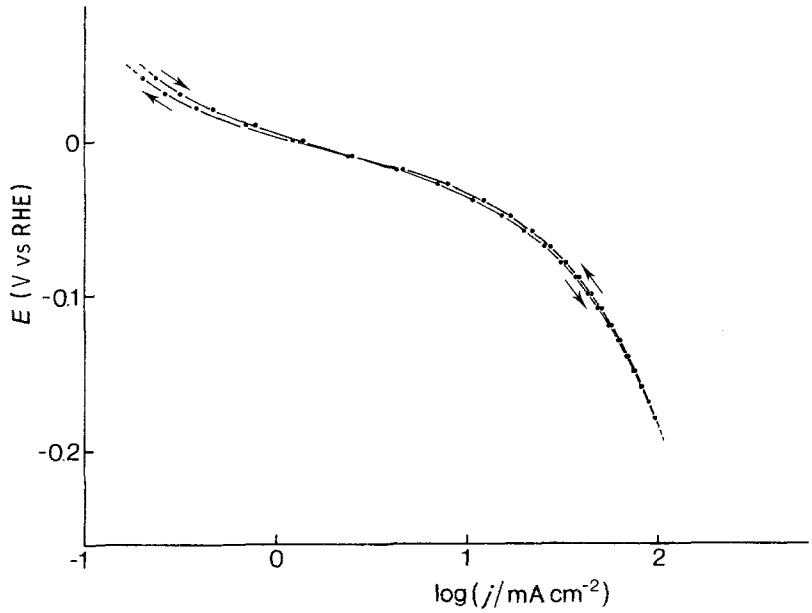


Fig. 2. Typical $E$–log $j$ curve for hydrogen evolution on $IrO_x$ from $HClO_4$ solution without any significant hysteresis.

has been shown to occur, for instance, with Ru [14] and Pt [15], i.e. with precious metals. A requirement is the presence of active atomic hydrogen as generally occurs on such metals. In the present case $ClO_4^-$ reduction cannot be totally ruled out, but the concentration of $HClO_4$ is not so high as to give serious interferences. Otherwise, especially the reaction order determination would be affected, which does not appear to be the case here.

The surface of $IrO_x$ must reach a well-defined state before giving reproducible results. This is thought to be related to wetting phenomena and not to surface modifications. Thermal oxides are not immediately wetted by the solution everywhere in cracks and pores; the mechanism of hydrogen evolution appears to promote wetting of the surface. This can be inferred from the experimental observations outlined below.

### 3.1. *Tafel plots*

'Up' and 'down' Tafel lines showed occasional hysteresis which reduced with the number of runs. A typical curve is shown in Fig. 1. The shape indicates that at high currents in the forward direction the solution probably spreads over the surface giving rise to sections of the $E$–log $j$ curve with lower slope than at lower overpotential. Simultaneously, it was observed with such electrodes that at the higher currents the hydrogen bubbles tend to grow and stick on the surface. If the curves were recorded up and down three to four times, no further hysteresis was observed and reproducible results were obtained. Under similar circumstances, any departure of overpotentials from the low $\eta$ Tafel line turns out to be entirely attributable to ohmic drops. Therefore, in the hydrogen evolution region up to about 0.1 A cm$^{-2}$ apparent current density is characterized by a single Tafel line, as shown in Fig. 2.

### 3.2. *Surface charge*

The voltammetric charge, $q^*$, has been observed to increase with the number of runs up to a maximum value. The largest increase with respect to freshly prepared electrodes has been recorded after the first set of experiments. Figure 3 shows that a linear relationship exists between $q^*$ for fresh electrodes and $q^*$ for the same electrodes after the first hydrogen evolution experiments. In the high $q^*$ range (large surface area electrodes) the charge has been observed to increase by a factor of about 1.7. However, in the low $q^*$ range (smoother electrodes), the increase is only 1.4. This indicates that the increase is lower especially for the high-temperature oxides which are expected to be more hydrophobic. Gas bubbles should adhere more to non-wetted surfaces.

After the second set of hydrogen evolution experiments the charge $q^*$ increases further by only about 20%. In the high $q^*$ range the slope is now 0.5 (Fig. 3), which means that the charge is twice the initial one. Such a charge was not observed to appreciably increase further. The electrodes were then stored in two different groups: one in the laboratory air and the other in pure water. After *ca* 3 months of storage, the former set of electrodes showed a somewhat lower charge, while in the latter set the charge remained remarkably constant. This suggests that some de-wetting of the surface can take place in air; this is prevented by keeping the electrode in water.

A ratio of 2 between charges measured in different conditions is not unusual with oxide electrodes. Thus, a ratio of 0.5 has been found between $q^*$ in neutral unbuffered solutions and $q^*$ in strongly acid and alkaline media [8, 16], as well as between $q^*$ measured with fast transients and $q^*$ at steady state [17]. This has been attributed to the difference between the macroscopic outer surface and the total surface including difficult-to-reach regions. Thus, wetting of the inner surface is apparently promoted by hydrogen evolution which enables the solution to spread by changing hydrophobic into hydrophilic sites. As will be shown later, the modification is probably accomplished via a reduction and reoxidation of the oxide surface.

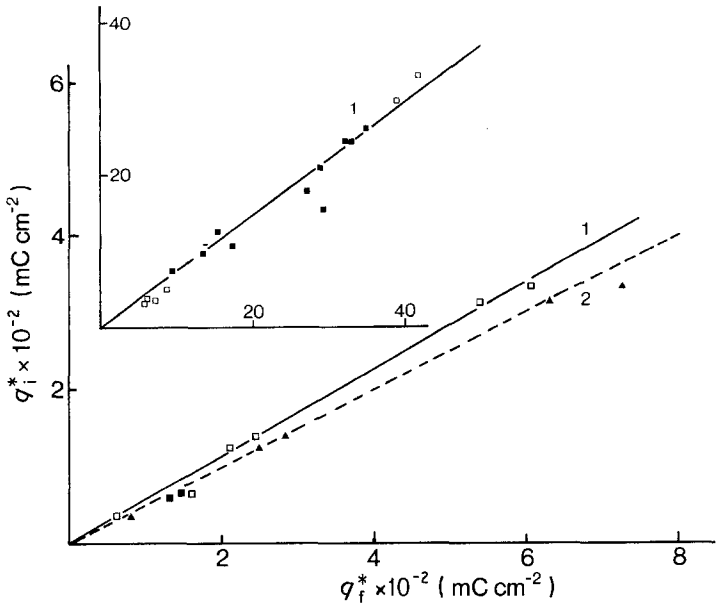


Fig. 3. Voltammetric charge for fresh $IrO_x$ electrodes ($q_i^*$) against the charge after the first (1, □) and the second (2, ▲) hydrogen evolution experiment ($q_f^*$). Inset: the same plot (1) in the low-charge region. (■) Different set of electrodes no longer used.

### 3.3. *Apparent exchange current*

It is often thought that pores, such as those present in thermally prepared oxides, should be blocked by gas evolution reactions. However, it has been shown that the pores work in $O_2$ evolution [11], while they do not in $Cl_2$ evolution [17]. The reason is that $Cl^-$ is sparingly supplied into pores by diffusion, while $O_2$ is evolved from water by a mechanism which does not deplete the pores of the solvent. Figure 4a shows a plot of the apparent exchange current as a function of $q^*$. A linear relationship with unit slope results. Since $q^*$ measures the active surface [11, 18], the outcome indicates that hydrogen evolution takes place on the whole active surface even with the most porous (or rough) electrodes.

Although the charge varies from the first to the second set of experiments, the apparent exchange current in the forward scan does not change substantially. This is shown in Fig. 4b where for the same electrodes as in 4a a linear relationship of unit slope between the two quantities can be seen. The points are admittedly scattered but this is especially true precisely for those electrodes still showing hysteresis. Thus, once most of the available surface has been wetted, the low-overpotential behaviour is thought to be representative of the kinetics of the process.

The situation is different for the apparent exchange current measured during the backward scan in the second set of experiments. Figure 5a shows a plot of $(j_0)_b$ against the appropriate surface charge $q^*$. The relationship is still probably linear but the slope is now different from 1 and much higher. If $(j_0)_b$ is plotted against $(j_0)_f$ for the same 'up and down' curve, Fig. 5b shows that apart from some scattered points, the relationship is linear but the slope is higher than 1. Quantitative comparison between $j_0$ values for particular electrodes shows that they are almost the same for high $q^*$ electrodes while the difference increases systematically as $q^*$ decreases. The results indicate that the activation of the surface by hydrogen evolution is a regular function of $q^*$, increasing as $q^*$

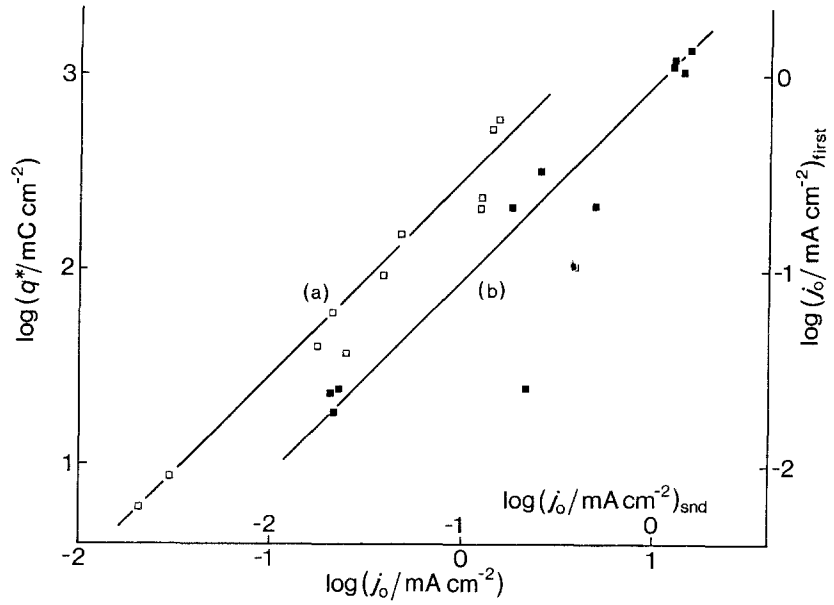


Fig. 4. (a) Dependence of the exchange current for the hydrogen reaction on the voltammetric charge of the $IrO_x$ electrodes. (b) Exchange current for the first set of experiments against the exchange current for the second set (forward direction).

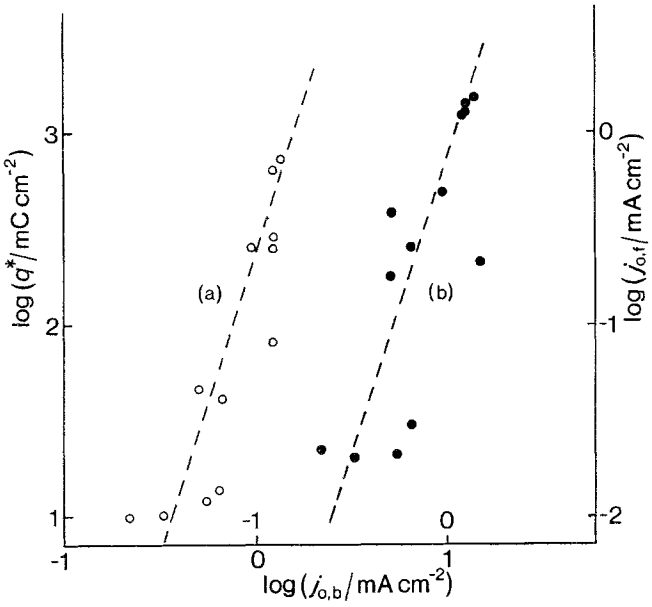


Fig. 5. (a) Exchange current (backward direction) for hydrogen evolution on $IrO_x$ electrodes against the voltammetric charge. (b) Exchange current (forward direction) against exchange current (backward direction) in the second set of experiments of hydrogen evolution on $IrO_x$ electrodes.

decreases. It thus appears that $(j_0)_b$ may not be representative of a steady state situation during the second set of hydrogen evolution experiments.

### 3.4. *Tafel slopes*

It has been mentioned above that hydrogen evolution takes place with a single Tafel line up to about $0.1\,A\,cm^{-2}$, the high current limit adopted in this work. Figure 6 shows a plot of the Tafel slope against the surface charge. $b$ varies between narrow limits from *ca* 35 mV to *ca* 50 mV. It is seen that $b$ tends to increase as $q^*$ is reduced, a trend already observed with $RuO_x$ in $O_2$ and $Cl_2$ evolution [11, 19]. The explanation given previously for the case of $Cl_2$ can be extended to the present case. Thus, in view of the high activity for hydrogen evolution (note that the apparent exchange current for the most active electrode is of the same order of magnitude as that for $Cl_2$ evolution on $RuO_x$) it is possible that the Tafel slope is decreased towards 30 mV by some slow removal of the $H_2$ produced at the surface [19, 20]. The high $b$ limit might indicate a trend towards a change in mechanism, but this is not supported by the order of reaction (see later).

In Fig. 6 the Tafel slopes of the backward curves are also reported. They are systematically lower than those for the forward scans, i.e. the electrodes show higher activity. Since they vary from *ca* 32 mV to *ca* 40 mV as $q^*$ decreases, it is thought that a Tafel slope of 40 mV is probably the most realistic one to represent the kinetics of the reaction. No kinetic significance can be attached to the slight increase at low $q^*$ which in the forward scan is probably related to some wetting–dewetting residual phenomena.

The reasonableness of a Tafel slope of 40 mV as representative of the process emerges more clearly from Fig. 7 where $b$ is plotted against the calcination temperature. $b$ is seen to be around 35 mV for the most active electrodes (calcined between 330 and 400° C) while large differences between $b_f$ and $b_b$ can be noticed at higher temperatures than 400° C where the phenomenon of thermal dewetting of the surface becomes more important.

### 3.5. *Ohmic drop*

The ohmic drop component is an important parameter with oxide electrodes because of its relation to the state of the support/active layer interface. Figure 8

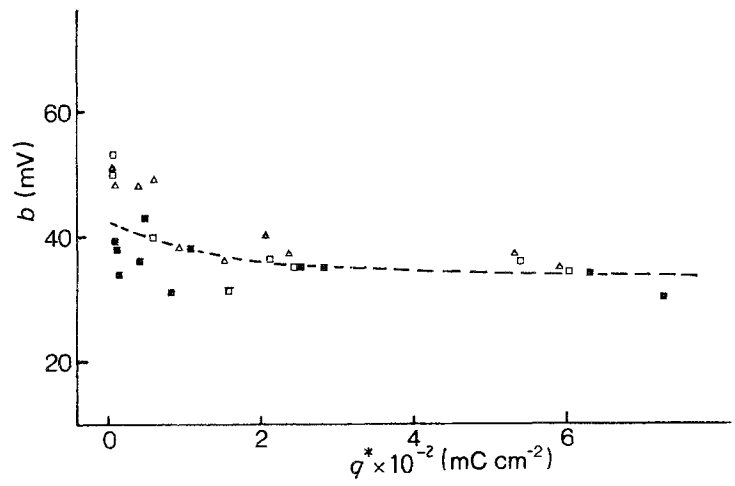


Fig. 6. Tafel slope for hydrogen evolution from acid solution on $IrO_x$ electrodes as a function of the voltammetric charge. (△) First set of experiments. Second set of experiments: (□) forward and (■) backward direction. (– – –) Apparent dependence.

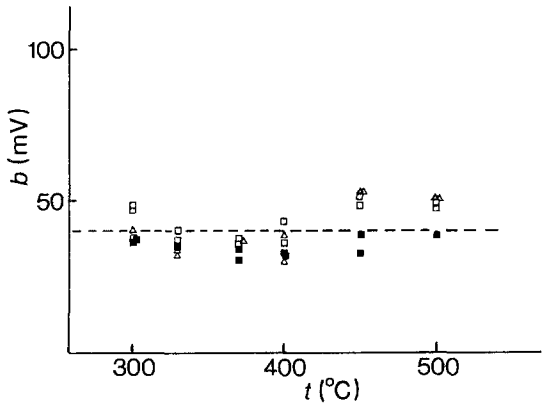


Fig. 7. Dependence of Tafel slope for hydrogen evolution from acid solution on $IrO_x$ electrodes on the oxide calcination temperature. (△) First set of experiments. Second set of experiments: (□) forward and (■) backward direction.

shows the average resistance at the electrode surface as derived from *IR* drop corrections to the Tafel lines. *R* is seen to depend on the calcination temperature at the two extremes of the range. Thus *R* rises sharply at temperature higher than 450° C, and this can be explained in terms of the growth of an insulating film on the Ti support during firing.

At 300° C *R* is also slightly higher. At this temperature the thermal decomposition is hardly complete and the layer may be partly in a reduced state. $Ir_2O_3$ is known [21, 22] to be a poor conductor with respect to $IrO_2$ and may well be responsible for the small increase in the layer resistance. However, this does not appear to influence the reaction mechanism.

Between 330 and 450° C, *R* has been measured to be between 0.5 and 1 Ω. This is a 'normal' value for the cell used in this work and is entirely attributable to the solution resistance. This result suggests that hydrogen evolution is not accompanied by solid state reduction of the oxide as appears to happen with electrolytically grown oxides. Thus, intermediate adsorption involves only the top monolayer of the oxide surface. This explains why the surface charge, $q^*$ is completely recovered even after prolonged hydrogen evolution. Experiments showed that the voltammetric

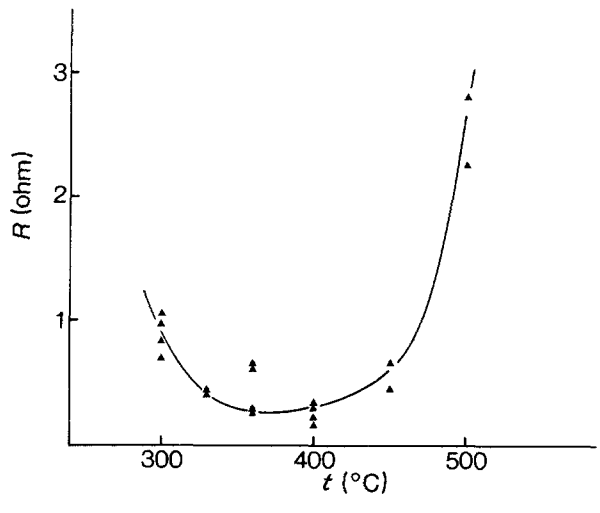


Fig. 8. Dependence of the ohmic drop correction on the calcination temperature of $IrO_x$ electrodes.

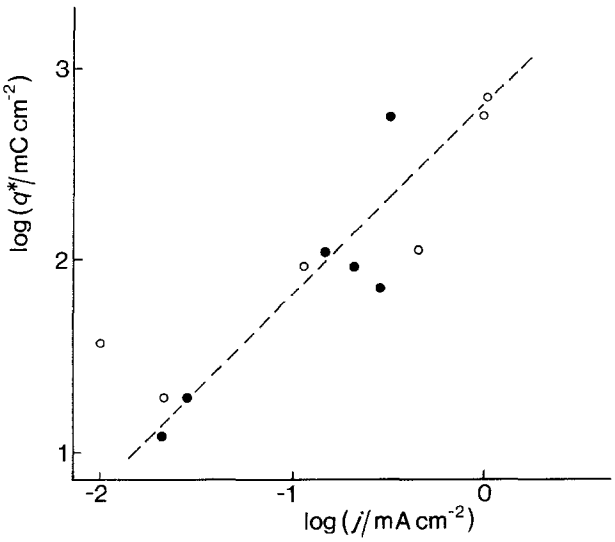


Fig. 9. Correlation between voltammetric charge and the average current for hydrogen evolution on $IrO_x$ in reaction order determinations. (○) Forward potential step; (●) backward potential step.

curve became asymmetric after cathodic treatment ($q_a^* > q_c^*$) but just after one voltammetric cycle the normal balance was observed ($q_a^* = q_c^*$) although the total value of $q^*$ increased.

A detailed voltammetric study of the cathodic behaviour of thermal $IrO_x$ will be reported in a forthcoming paper.

### 3.6. *Reaction order*

In view of the wetting–dewetting behaviour of the surface, the reaction order was determined both forwards and backwards as described in Section 2.4. No quantitative difference was observed. Since the charge did not increase appreciably before and after the set of measurements, the electrodes were probably in reproducible wetting conditions. In fact, Fig. 9 shows that the charge dependence of the current exhibits the same pattern for both backward and forward potential steps, unlike the situation depicted in Fig. 5b.

Figure 10 shows that ${}_\eta\nu(H^+)$, the reaction order at constant overpotential, is strictly zero for all electrodes in the acid pH range investigated. Thus, with a Tafel slope of 40 mV, hence a transfer coefficient equal to $(1 + \alpha_c)$, the chemically significant reaction order, i.e. the reaction order at constant potential is:

$$ {}_E\nu(H^+) = {}_\eta\nu(H^+) + (1 + \alpha_c) = (1 + \alpha_c) \quad (1) $$

It follows that ${}_E\nu(H^+)$ has a fractional value around 1.5.

Fractional reaction orders have been observed with $RuO_x$ in oxygen evolution [23, 24] and have been explained in terms of surface acid–base equilibria [24, 25]. More specifically, as the pH of the solution is changed, the potential $\phi^*$ at the reaction plane shifts according to the equation:

$$ \phi^* = -(RT/F)\mathrm{pH} \quad (2) $$

Once introduced into the kinetic equation to correct

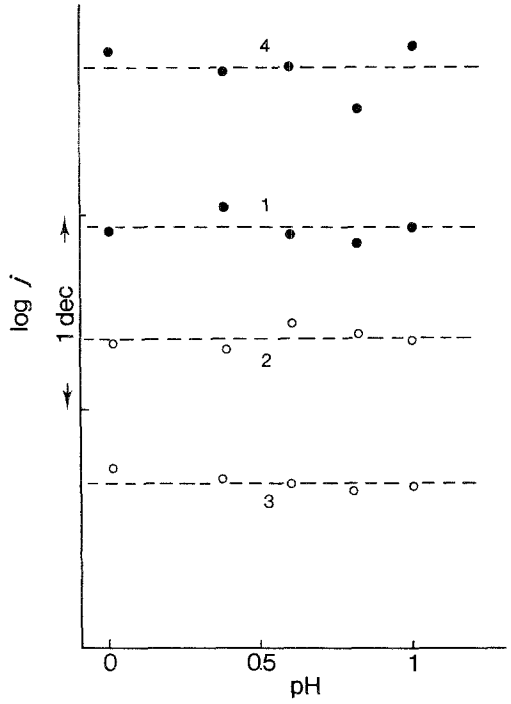


Fig. 10. Dependence of current at constant overpotential on pH for hydrogen evolution on $IrO_x$ electrodes from 1 mol dm$^{-3}$ ($NaClO_4$ + $HClO_4$) solutions. (○) Forward direction; (●) backward direction. Electrodes: (1) 300; (2) 400; (3) 450; (4) 500° C.

the electrode potential Equation 2 changes the reaction order of $H^+$ by $\alpha$ [25]. Therefore, the true chemically significant reaction order, not distorted by double layer effects, is 1.

### 3.7. *Reaction mechanism*

As usually happens with oxides [19, 26], the known classical reaction mechanisms are unable to reproduce the observed kinetic parameters. This has been the case for $O_2$ and $Cl_2$ evolution on a number of transition metal oxides [27] and is also the case for $IrO_x$ in hydrogen evolution.

The classic mechanism predicting 40 mV Tafel slope is the following:

$$H^+ + e \longrightarrow H_{ad} \qquad (3a)$$

$$H_{ad} + H^+ + e \longrightarrow H_2 \qquad (3b)$$

with Step 3b being rate determining. However, the same mechanism requires an order of reaction of 2 with respect to $H^+$ which has not been observed. Since the second electron transfer must be slow, $H^+$ must appear only once, either in the first or in the second step but not in both.

It has been proposed for anodic reactions that one of the steps should involve the oxidation of the active sites [24]. By analogy, for cathodic reactions one of the steps may be the reduction of the active sites. Thus, the following mechanism is proposed here:

$$M\text{–}OH + H^+ + e \longleftrightarrow M\text{–}OH_2 \qquad (4a)$$

$$M\text{–}OH_2 + e \longrightarrow M\text{–}H + OH^- \qquad (4b)$$

$$M\text{–}H + H_2O \longleftrightarrow M\text{–}OH + H_2 \qquad (4c)$$

The kinetic equation is:

$$j_c \sim [M\text{–}OH_2] \exp[-\alpha_c F(E - \phi^*)/RT] \qquad (5)$$

Considering the equilibrium for Step 4a and introducing Equation 2, Equation 5 becomes:

$$j_c \sim [H^+]^{1+\alpha} \exp[-(1 + \alpha_c)FE/RT] \qquad (6)$$

which shows the origin of the fractional reaction order. Concentration profiles for $H^+$ (double layer effects) are not to be taken into account since solutions at constant ionic strength have been used.

M–OH is the characteristic site of an oxide surface [28]. $M\text{–}OH_2$ represents the surface complex of a 'reduced' site. The exact nature is not known and only occasionally is it here coincident with the formula of water. It may be so, but no data are thus far available to chemically identify the intermediate.

Step 4c is a chemical reaction which is normally not considered to take place on metal surfaces. However, it may be accelerated in this case by the formation of the M–OH surface bond which decreases the activation energy. On the other hand, after prolonged discharge the oxide electrode is observed to lose all adsorbed hydrogen rather easily since the original open circuit potential is rapidly recovered. In the presence of bubbling $H_2$ gas, the equilibrium potential of the hydrogen electrode is not observed. This indicates that $H_2$ does not dissociate on the surface and no equilibrium justifying a step such as:

$$M\text{–}H + M\text{–}H \longrightarrow M + H_2 \qquad (4d)$$

is established. On the other hand, Step 4d does not close the reaction cycle, and in addition it requires some surface intermediate diffusion which is hampered on oxide surfaces by the OH groups.

The exact nature of Step 4c is not relevant to the kinetic parameters, so a kinetically equivalent mechanism could be the following:

$$M\text{–}OH + H^+ \longleftrightarrow M\text{–}OH_2^+ \qquad (7a)$$

$$M\text{–}OH_2^+ + e \longleftrightarrow M\text{–}OH_2 \qquad (7b)$$

$$M\text{–}OH_2 + e \longrightarrow M\text{–}H + OH^- \qquad (7c)$$

Mechanism 7 differs from 4 in that active sites are only those where $H^+$ is adsorbed and not the whole surface. However, in this case the number of active sites is pH dependent and the final result is the same as for Mechanism 4.

## 4. Conclusions

(a) $IrO_x$ is a good electrocatalyst for hydrogen evolution. On the most active electrodes the apparent exchange current is of the order of $10^{-3}$ A cm$^{-2}$, so the overpotential is only about 0.1 V at 10 kA m$^{-2}$ (1 A cm$^{-2}$). So high an activity is comparable to that of $RuO_x$ for $Cl_2$ evolution. However, the $Cl_2$ reaction is reversible and with bubbling $Cl_2$ the oxide electrodes take the equilibrium potential. This is not the case for the $H_2$ reaction despite the high apparent current density. The reason is that the 'reduced' sites, necessary for the establishment of the equilibrium, can only

be formed electrochemically and not by $H_2$ dissociation.

(b) The formation of the 'reduced' sites promotes the wetting of the electrode surface, a prerequisite for the liberation of normally sized gas bubbles. Otherwise, large bubbles stick on the surface and hysteresis phenomena, which distort the Tafel lines, are observed. In addition, pores are excluded on dewetted (hydrophobic) surfaces. The extent of wetting–dewetting phenomena appear to depend on the magnitude of current. This means that the apparent activity may be different depending on the direction of electrode potential application. Long-term performances need to be investigated in this respect.

(c) Anodically grown oxides are usually reduced in the bulk during cathodic polarization. $IrO_x$ anodic films show the formation of non-conducting $Ir_2O_3$ at cathodic potentials before hydrogen evolution [21, 22]. This is not the case for thermal $IrO_x$. No ohmic drop components other than that on the solution side are observed during hydrogen evolution. This indicates that the reaction involves only the very surface of the oxide and the lattice is never modified. Reasons for this are to be sought in the metallic conductivity of $IrO_x$: since no electric field penetrates into the crystal, ionic motion necessary for bulk reduction is prevented, despite the established thermodynamic unstability. However, since reduction to the metal also seems to be slow for dissolved complexes (Ir does not plate with good current efficiency), other factors besides the electronic conductivity might be responsible for the cathodic stability of $IrO_x$.

(d) The mechanism of hydrogen evolution differs by a different reaction order from the classic one predicting the same Tafel slope. Ths is due to the involvement of the active site reduction as one of the steps in the mechanism. A fractional reaction order is observed for $H^+$ which can be explained in terms of the known acid–base response of an oxide surface to pH [28]. This provides further support to the view that the surface is never 'like that of the metal' even during strong hydrogen evolution. It also explains the dramatically different adsorption properties observed with Ru and $RuO_x$ in respect to metallic impurities present in solution [5].

## Acknowledgements

J. F. C. Boodts thanks the CNPq (Brasilia) for a fellowship financing his visit to Milan. S. Trasatti acknowledges the financial support to this work by the C.N.R. (Rome).

## References

[1] J. F. Cairns, D. A. Denton and P. A. Izard, Eur. Pat. Appl. EP 129, 374 (1984); *Chem. Abstr.* **102** (1985) 102442.
[2] A. Nidola, PCT Int. Appl. WO 86 03, 790 (1986); *Chem. Abstr.* **105** (1986) 122974.
[3] H. Debrodt, Eur. Pat. Appl. EP 129, 088 (1984); *Chem. Abstr.* **102** (1984) 122040.
[4] D. Galizzioli, F. Tantardini and S. Trasatti, *J. Appl. Electrochem.* **5** (1975) 203.
[5] E. R. Kötz and S. Stucki, *J. Appl. Electrochem.* **17** (1987) 1190.
[6] T. Hepel, F. H. Pollak and W. E. O'Grady, *J. Electrochem. Soc.* **131** (1984) 2094.
[7] T. Hepel, F. H. Pollak and W. E. O'Grady, *J. Electrochem. Soc.* **132** (1985) 2385.
[8] S. Trasatti and G. Lodi, in 'Electrodes of Conductive Metallic Oxides, Part A' (edited by S. Trasatti), Elsevier, Amsterdam (1980) p. 301.
[9] R. Kötz and S. Stucki, *Electrochim. Acta* **31** (1986) 1311.
[10] R. Garavaglia, C. M. Mari and S. Trasatti, *Surf. Technol.* **23** (1984) 41.
[11] G. Lodi, E. Sivieri, A. De Battisti and S. Trasatti, *J. Appl. Electrochem.* **8** (1978) 135.
[12] S. Ardizzone, A. Carugati and S. Trasatti, *J. Electroanal. Chem.* **126** (1981) 287.
[13] R. Boggio, A. Carugati, G. Lodi and S. Trasatti, *J. Appl. Electrochem.* **15** (1985) 335.
[14] F. Colom and M. J. Gonzalez-Tejera, *J. Electroanal. Chem.* **190** (1985) 243.
[15] G. Horanyi and G. Vértes, *J. Electroanal. Chem.* **64** (1975) 252.
[16] L. D. Burke, O. J. Murphy, J. F. O'Neil and S. Venkatesan, *J. Chem. Soc. Faraday Trans. 1* **73** (1977) 1659.
[17] S. Ardizzone, A. Carugati, G. Lodi and S. Trasatti, *J. Electrochem. Soc.* **129** (1982) 1689.
[18] B. Aurian-Blajeni, A. G. Kimball, L. S. Robblee, G. L. M. K. S. Kahanda and M. Tomkiewicz, *J. Electrochem. Soc.* **134** (1987) 2637.
[19] S. Trasatti, *Electrochim. Acta* **32** (1987) 369.
[20] V. V. Losev, *Elektrokhimiya* **17** (1981) 733.
[21] B. E. Conway and J. Mozota, *Electrochim. Acta* **28** (1983) 9.
[22] L. D. Burke and D. P. Whelan, *J. Electroanal. Chem.* **162** (1982) 121.
[23] A. Carugati, G. Lodi and S. Trasatti, *Mater. Chem.* **6** (1981) 255.
[24] L. I. Krishtalik, *Electrochim. Acta* **26** (1981) 329.
[25] C. Angelinetta, M. Falciola and S. Trasatti, *J. Electroanal. Chem.* **205** (1986) 327.
[26] S. Trasatti, in 'Electrochemical Hydrogen Techniques' (edited by H. Wendt), Elsevier, Amsterdam (in press).
[27] V. Consonni, S. Trasatti, F. Pollak and W. E. O'Grady, *J. Electroanal. Chem.* **228** (1987) 393.
[28] A. Daghetti, G. Lodi and S. Trasatti, *Mat. Chem. Phys.* **8** (1983) 1.